

# Intact and broken cellulose nanocrystals as model nanoparticles to promote dewatering and fine-particle retention during papermaking

Connor J. Lenze · Caryn A. Peksa · Weimin Sun · Ingrid C. Hoeger · Carlos Salas · Martin A. Hubbe

Received: 23 May 2016 / Accepted: 26 September 2016 / Published online: 28 September 2016  
© Springer Science+Business Media Dordrecht 2016

**Abstract** Cellulose nanocrystals (CNCs), either in intact form or after mechanical shortening, were used as a model nanoparticle for enhancement of dewatering and fine-particle retention during lab-scale papermaking process evaluations. Cryo-crushing, using dry or wet CNCs, was performed to shorten the particles from an initial mean value of 103.1 nm to either 80.4 nm (wet crushed) or 63.4 nm (dry crushed). Papermaking-related tests were performed with the solids from 100 % recycled copy paper, which were prepared as a 0.5 % solids suspension in dilute Na<sub>2</sub>SO<sub>4</sub> solution and then treated successively with 0.05 % of poly-diallyldimethylammonium chloride, 0.05 % of very-high-mass cationic acrylamide copolymer, and then various types and dosages of negatively charged nanoparticles. The performance of the CNCs, relative to papermaking goals, was compared to that of two colloidal silica products that are widely used in industry for this purpose. All of the nanoparticles were observed to promote both

dewatering and fine-particle retention. The intact CNCs were more effective than the broken CNCs with respect to fine-particle retention. Effects on flocculation of the fiber suspension were detectable, but not large relative to the sensitivity of the test employed. Results are discussed in the light of concepts of polyelectrolyte bridges and the participation of elongated nanoparticles in completing those bridges in such a way as to form shear-sensitive attachments among solids surfaces in the suspension.

**Keywords** Paper machine chemical programs · Drainage aids · Retention aids · Microparticles · Nanocellulose · Colloidal silica

## Introduction

Nanoparticle-based and microparticle-based additive systems have been widely used within the paper industry since the 1980s as a means of achieving favorable combinations of the rate of water release, fine-particle retention, and uniformity of formation during the preparation of a paper sheet (Andersson et al. 1986; Langley and Litchfield 1986; Breese 1994; Anderson and Lindgren 1996; Hubbe 2005). In particular, it has been found that higher rates of drainage, including water release assisted by hydrofoil action and vacuum, can be achieved by such programs (Andersson et al. 1986; Langley and Litchfield 1986;

---

C. J. Lenze · C. A. Peksa · W. Sun · I. C. Hoeger · C. Salas · M. A. Hubbe (✉)  
Department of Forest Biomaterials, North Carolina State University, Campus Box 8005, Raleigh, NC 27695-8005, US  
e-mail: hubbe@ncsu.edu

W. Sun  
Department of Applied Chemistry, School of Science, Northwestern Polytechnical University, 127 Youyi Xilu, Xi'an 710072, Shaanxi, China

Swerin et al. 1995; Wågberg et al. 1996; Harms 1998). The most widely used particulate additives to promote dewatering and fine-particle retention are colloidal silica (Swerin et al. 1995; Anderson and Lindgren 1996; Sang et al. 2012) and sodium montmorillonite, which is often called “bentonite” (Langley and Litchfield 1986; Asselman and Garnier 2001). Certain highly cross-linked anionic polyelectrolyte products also have been used, and similar effects have been reported (Honig et al. 2000). One of the distinguishing features of these widely used systems is that they depend on a strong interaction between the negative charge at the micro- or nano-particle surface and the positive charge of a very-high-mass cationic polyelectrolyte (Hubbe 2005; Swerin et al. 1993). It is very common for the micro- or nano-particle to be added as late as possible to the system, just before the fiber suspension is formed into paper (Langley and Litchfield 1986). Alternatively, it is also common to invert the order of addition, mixing the micro- or nanoparticle additive with the fiber suspension just before addition of a cationic flocculant, after which the suspension is almost immediately formed into paper.

In the 1990s some published articles announced the development of a class of new “structured” colloidal silica products for papermaking applications (Moffett 1994; Andersson and Lindgren 1996; Harms 1998; Main and Simonson 1999). Unlike the colloidal silica products used up to that time as papermaking additives, the new products were comprised of irregular chains of fused primary  $\text{SiO}_2$  nanoparticles, i.e. the “gel” form of colloidal silica particles. It was stated that such products would be inherently more effective for promotion of fine-particle retention, while still having a strong ability to promote dewatering. The enhanced capability was attributed to the high aspect ratio of the gel type of colloidal silica.

Recently, cellulose nanocrystals (CNCs) have become widely available in quantities suitable for laboratory research and pilot-scale development (Reiner and Rudie 2013; Zhang et al. 2013). The availability of these materials provides an opportunity to use them as a model nanoparticle, as a means to probe some aspects of the mechanism by which certain dewatering and fine-particle retention programs function (Xu et al. 2014). CNCs offer the advantages of having a simpler geometry in comparison to structured colloidal silica (gel-type) products, as well as having a relatively narrow length distribution. CNCs, when

produced using concentrated sulfuric acid, also resemble colloidal silica (Sears 1956) in having a strongly negative surface charge when immersed in water (Araki et al. 1998, 1999; Habibi 2010; Abitbol et al. 2013). In this work, CNCs having different mean lengths were used for the first time in a study of the papermaking process.

## Experimental

### Nanoparticles

The CNCs used in this work were all based on the spray-dried CNC powder (Item No. 6) supplied by the University of Maine (<http://umaine.edu/pdc/process-and-product-development/selected-projects/nanocellulose-facility/nanocellulose-requests/>). As is well known, this material is prepared at the Forest Product Laboratory, Madison, Wisconsin, by digestion of cellulose in concentrated sulfuric acid, thus giving rise to particles that have sulfate groups at their surfaces (Habibi 2010; Abitbol et al. 2013). The product is known to be prepared with  $\text{Na}^+$  as the associated cation. Upon placement in water, the ionizable groups at the cellulosic surfaces contribute to rapid wetting, as well as good dispersion in water on account of the repulsive electrostatic forces between adjacent particles.

Crushing of the CNC was carried out by chilling the nanoparticles to liquid nitrogen temperature. Two batches of crushed CNCs were prepared. The first batch (dry crushed) was prepared by adding 1.5–2 mm<sup>3</sup> of dry CNC powder (no packing pressure applied) into the cell of a Model 6750 Freezer/Mill cryo-crushing device supplied by SPEX Certiprep, Metuchen, NJ, USA. The device was run for two standard cycles of 5 min each. The full procedure was done again the same way, but with a 10 % slurry of CNC in water (wet crushed), such that a frozen combination of water–ice and CNC particles was crushed together.

Micrographs of representative particles from the intact and crushed CNC batches were obtained by atomic force microscopy (AFM). In preparation, silicon wafers (1 cm × 1 cm) were cleaned with water, then ethanol, followed by exposure to UV and ozone. The wafers were then immersed in a 500 ppm solution of poly-ethyleneimine (PEI), followed by rinsing with water. A dilute suspension of 0.01wt % CNCs (of each

type) in water was prepared by sonication at 10–30 % amplitude of a Branson Digital Sonifier, Model No. 102C (CE) device for about 30 s, and then placed dropwise onto a PEI-treated wafer and allowed to dry. AFM tests were carried out with a NanoScope III D3000 device from Digital Instruments Inc.

For comparison purposes, two widely used industrial products were included in the experiments, representing the “gel” (structured) and “sol” (singlet particles) types of colloidal silica (Andersson and Lindgren 1996; Harms 1998). Product NP 320, a structured colloidal silica product obtained from Kemira, has been described as consisting of irregular chains of fused nano-sized primary silica particles. The primary particles are understood to be spheres having diameters near to 2–4 nm. Those primary particles are fused together into irregular chains or extended clusters having lengths in the range of about 10–60 nm. Product NP 440 was selected as a representative for non-structured silica. The particles of NP 440 are understood to be spheres having diameters of about 5 nm. Such products have been discussed and characterized in other studies (Carlson 1990; Andersson and Lindgren 1996; Harms 1998; Hagen and Tokarz 2002; Carr 2005).

The surface charge of each type of nanoparticle was evaluated by streaming current tests, using a PCD-pH device from BTG Corp. After rinsing the equipment, 10 mL of deionized water was combined with 1 ml of 1 % nanoparticle suspension and sufficient sodium carbonate to make a  $10^{-4}$  M buffer solution (pH  $\sim$  9.5) in order to convert any weak acidic groups to their anionic form. Four replicate titrations were carried out in each case using poly-DADMAC (see next).

### Preparation of cellulosic fiber and fine-particle suspensions

The pulp suspensions used throughout the work were prepared with fiber from 100 % recycled Enviro-copy® standard white copy paper (Office Depot) at a 0.5 % solid suspension level using a TAPPI disintegrator (TAPPI Method T 205). After resuspension of the paper solids into deionized water, giving a consistency of 0.5 %, sufficient sodium sulfate was added to achieve an electrical conductivity of 1000  $\mu$ S/cm at a laboratory temperature of approximately 22 °C. A confirmatory set of experiments

(evaluating the retention effects) was carried out at 2000  $\mu$ S/cm; since the main effects were generally the same at the two conductivity levels, only the results corresponding to 1000  $\mu$ S/cm are reported in this work. The adjustment of electrical conductivity is important so that the system can be representative of salt ion levels that are likely to be encountered in paper manufacturing facilities. Due to the presence of calcium carbonate filler in the recycled paper, the pH of the suspensions was in the range of 8–8.5.

Before being mixed with the pulp suspension, all nanoparticle materials (i.e. either CNCs or colloidal silica) were pre-diluted to 1.0 % solids to facilitate volumetric measuring and efficient mixing with the pulp suspensions. The poly-DADMAC (Aldrich Cat. No. 40, 901-4, low mass, supplied as 20 % solids solution) was prepared as a 1.0 % solution in water. The cationic acrylamide copolymer (Percol® 175, BASF, dry bead form) was prepared as a 0.1 % solution.

### Rate of water release during papermaking

Rates of water release from differently treated fiber suspensions were evaluated using a modified Schopper–Riegler test device (Sampson and Kropholler 1995; Sampson 1997). This device differs from a standard Schopper–Riegler tester with respect to its base. Rather than having the filtrate pass through a capillary opening at the base of the collection funnel, there was a large opening, allowing immediate flow of the filtrate into a tared beaker resting on an electro-balance. Also, the device had no “side arm” for collection of filtrate. Such a modified system offers two advantages when used for research work that involves the addition of polyelectrolytes such as cationic acrylamide copolymer (cPAM). First, the results are easier to interpret. Secondly, any high-mass polyelectrolyte present in the aqueous phase would be expected to markedly slow down the flow through a capillary (Sridhar et al. 1991; Larson 2005), and such issues are avoided by the modified system.

To run an individual test, 1000 ml of optionally treated fiber suspension, having a consistency of 0.5 % and a conductivity of 1000  $\mu$ S/cm, was prepared. In a large beaker, with continued stirring at 500 rpm, the suspension was treated first with 0.05 % poly-DADMAC solids (1 % solution concentration), followed by 30 s of continued agitation, then 0.05 %

cPAM solids (0.1 % solution concentration), followed by 30 s of continued agitation, then by nanoparticle suspension addition at an amount to be specified. The treated suspension then was placed at the top of the modified Schopper–Riegler device, while holding down a sealing cone. At time equal to zero, the sealing cone was allowed to spring upwards, by spring action, and simultaneously a timer was started. The amounts of filtrate accumulated in the tared beaker were recorded at elapsed times of 5, 10, 20, 30, 40, 50, and 60 s. These data were captured by videography, showing both the times and the output of a tared electronic balance. The reported mean values are based on four replicate tests of each condition. The 90 % confidence intervals for the observations were generally within the range of plus or minus 15 g from the mean values reported.

### Retention of fine particles during papermaking

To evaluate the effects of different nanoparticle treatments (following 0.05 % poly-DADMAC and 0.05 % cPAM) on the fine-particle retention, tests were carried out using a Dynamic Drainage/Retention Jar (Britt 1973; Britt and Unbehend 1976). The suspension was prepared in 500 ml batches having a consistency of 0.5 % in each case. An agitation speed of 500 rpm was used throughout all of the testing. In each case the first additive was poly-DADMC at the 0.05 % level based on solids. This was followed, after 30 s, by cPAM at the 0.05 % level. After an additional 30 s of agitation, the first portion of nanoparticles was added.

To allow for rapid collection and replication of data, turbidity was used as a means of quantifying the relative amounts of fine particulate matter (presumably mainly  $\text{CaCO}_3$  particles and cellulosic fines) present in the filtrate. Each turbidity measurement involved tenfold replication, using a DRT turbidimeter, Model 15CE. Filtrate was collected directly into the turbidimeter vial from the base of the Britt Jar device. The first portion was immediately placed back into the top of the jar, and tests were based on a second portion. The first replication of each test was obtained by gently inverting the capped vial, and then, after about 2 s, obtaining a new reading. Five such pairs of measurements were taken, with each pair of tests completed in about 60 s. In addition, each experimental run, as described above, was independently

repeated, providing either three or four replicate tests for evaluation of mean and standard deviation values.

Two series of tests were performed. In an initial full set of tests, after the poly-DADMAC and cPAM were in the system, the nanoparticles were added in successive amounts of 0.05 %, 0.05 % (for a net amount of 0.1 %), 0.1 % (for a net amount of 0.2 %), and 0.2 % (for a net amount of 0.4 %) with continuous stirring. A second series of tests was very similar except that a separate preparation involving poly-DADMAC and cPAM addition was carried out for each separate level of nanoparticle addition. In addition, a parallel series of tests in the continuous mode was carried out at an electrical conductivity of 2000  $\mu\text{S}/\text{cm}$ ; because the results showed basically the same trends, only the results of tests at 1000  $\mu\text{S}/\text{cm}$  are reported in this article.

### Fiber flocculation extent during papermaking

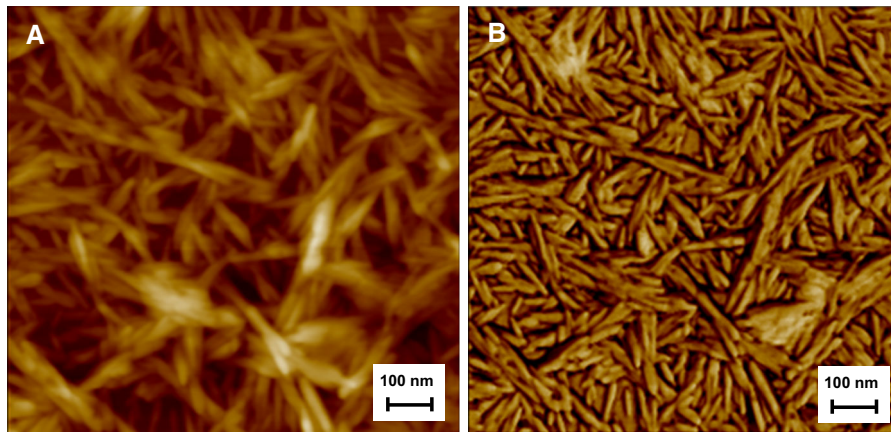
The extent of fiber flocculation, as a function of nanoparticle addition, was evaluated by means of a photometric dispersion analyser (PDA) from Rank Bros, Manchester, UK. A specialized “low gain” PDA version (Burgess and Phipps 2000; Hubbe 2000; Burgess et al. 2002) was employed in this work, allowing usage of a relatively large Tygon® tube (internal diameter ca. 6.35 mm) and the sensing of the state of flocculation in a 0.5 % consistency stock suspension. Each batch had a volume of 500 mL, and it was stirred continuously, using a magnetic stirrer at a rate just sufficient to prevent settling. A peristaltic pump was used to circulate the fibrous suspension from the beaker, through the PDA sensing zone, and back to the beaker, at a flow rate of 50 L/min. The gain setting was at 1.0 throughout the testing, and the output was selected as “RMS”, meaning the root-mean-squared of fluctuations in intensity of transmitted light through the tubing. In addition, the “filter” setting was selected in order to reduce the amount of noise in the output signal.

## Results and discussion

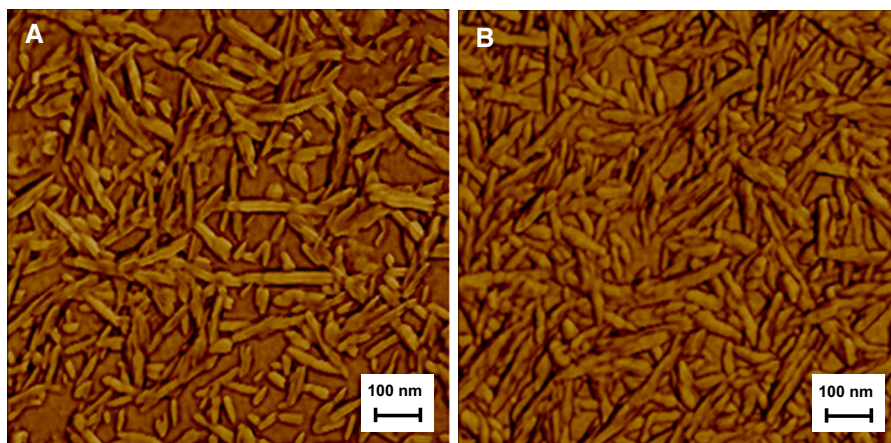
### Characterization of intact and broken CNC

Figure 1 shows atomic force micrographs of as-received CNC particles, comparing two modes of





**Fig. 1** Atomic force micrographs (AFM) of intact CNCs. **a**: Imaging based on height, with a sensing range of 40 nm. **b**: Imaging based on phase, using a 20° angle



**Fig. 2** AFM of two types of broken CNCs, with phase-based imaging. **a**: Batch 1, prepared under dry conditions (dry crushed). **b**: Batch 2, prepared with the freezing of a water suspension (wet crushed)

imaging. The depth-based image (Fig. 1a) provides a sense of the bulky nature of the layers of cellulosic material, with particles present in different planes. Because the phase-based images (as in Fig. 1b) were better resolved, those images were used as a means of estimating particle lengths. Because at least some of the observed particles can be at an angle to the plane of view, one can expect that there will be a systematic underestimation of CNC particle length based on measurements from the two-dimensional images. However, for the sake of making relative comparisons, it is assumed here that the degree of out-of plane orientation was similar for each of the samples evaluated. Based on visual measurements of 100 each representative CNCs appearing in the phase-based

images (Figs. 1b, 2a, 2b) the mean, standard deviation, and 90 % confidence interval for the intact and the broken CNC material were as shown in Table 1.

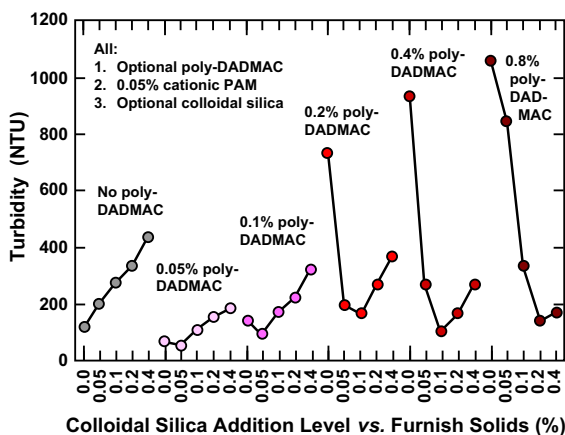
It is clear from these results that cryo-crushing can be regarded as an effective way to reduce the average length of CNCs. Secondly, the crushing achieved a greater reduction in size when the procedure was carried out in the absence of frozen water.

#### Optimization of treatment level for poly-DADMAC

Figure 3 shows results of a set of preliminary tests aimed at determining the optimum addition level of the highly cationic agent poly-DADMAC. In each

**Table 1** Length estimates (nm) of cellulose crystals

Description	Mean	SD	90 % confidence interval	
			Lower	Upper
Intact CNC	103.1	39.1	96.6	109.5
Wet crushed CNC	63.4	33.2	57.9	68.8
Dry crushed CNC	80.4	35.7	74.5	86.2

**Fig. 3** Optimization of poly-DADMAC level (on furnish solids) to achieve the lowest turbidity after subsequent treatment with 0.05 % cationic acrylamide copolymer, with final addition of different amounts of colloidal silica

case the poly-DADMAC addition was followed by 0.05 % of cPAM (based on solids vs. furnish solids) and then by sequential addition of four cumulative dosage levels of silica nanoparticles. Criteria for selection of an optimum set of treatments included achievement of a low turbidity value, consistent with very high retention of fine particles onto fibers, such that the filtrate passing through 76- $\mu$ m openings, which are too small to admit fibers, would be relatively free of particles. In addition, out of a concern to minimize costs, it is desirable to minimize the levels of both poly-DADMAC and the colloidal silica or other nanoparticle additive. Based on these criteria, the most favorable combination of results was achieved with a 0.05 % addition level of poly-DADMAC. This level was utilized in the subsequent work.

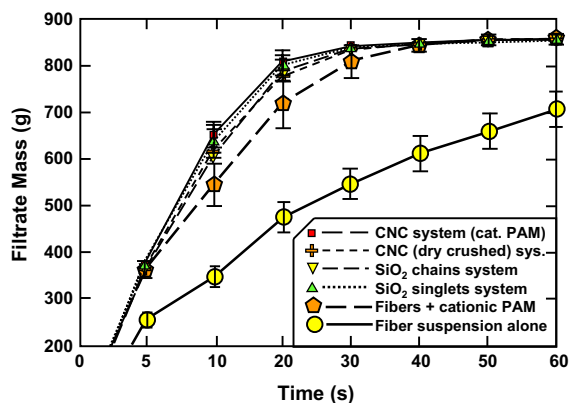
Based on previous work, there are two primary reasons to anticipate that a well-selected pretreatment with high-charge cationic polymer may lead to optimized performance of a nanoparticulate-based drainage-retention system. As has been shown

(Wågberg et al. 1996; Swerin et al. 1997), pretreatment with the high-charge polymer can favorably influence the adsorbed conformation of the high-mass cPAM added subsequently. Rather than lying down flat on the cellulosic surfaces, the cPAM is forced to adopt a more extended conformation having loops and tails extending from the surface into the solution phase. Secondly, a high-charge cationic polymer can be optimized to neutralize most of the excess of negatively charged polyelectrolytes, such as hemicellulose byproducts in solution, such that the more expensive cPAM is not wasted in complexing with such species.

It is notable in Fig. 3 that relatively high levels of poly-DADMAC pretreatment initially increased the filtrate turbidity, which is consistent with charge-reversal of the system. When cationic polyelectrolytes are in a sufficient excess, all of the wetted surfaces repel each other. Even in such an overdose situation, it was still possible to achieve relatively low values of turbidity by adding relatively large levels of negatively charged microparticles; however this would not be cost-effective.

#### Dewatering rates affected by nanoparticle addition

Figure 4 shows results of dewatering rate tests, using the modified Schopper–Riegler test device. As shown, the mass of filtrate collected as a function of time after initiating the drainage test depended strongly on whether or not cPAM (at the 0.05 % level, following

**Fig. 4** Filtrate mass as a function of drainage time in modified Schopper–Riegler test with 0.05 % poly-DADMAC, 0.05 % cPAM, and 0.4 % nanoparticles. Error bars indicate 90 % confidence intervals of the mean

0.05 % poly-DADMAC) had been added. It is notable that all of the conditions involving nanoparticles were clustered together, and all of them achieved an additional increment of drainage rate enhancement over what was achieved with just the cationic polymers.

The 90 % confidence intervals for this set of data typically extended about 16 g units from the plotted mean values. Therefore, one cannot conclude that any of the nanoparticles was more effective than another in promoting dewatering. The highest values were obtained with the default CNC, and this was closely followed by the sol-type (singlet) colloidal silica nanoparticle product. These results support the working hypothesis that cellulose nanoparticles can be utilized as a model to study the factors affecting retention and drainage programs.

As shown in Fig. 5, the mass of filtrate collected after 20 s of gravity drainage increased as a function of nanoparticle addition level (with the zero level corresponding to systems treated with poly-DADMAC and cPAM, at the same levels mentioned before). As already noted, based on statistical analysis one cannot conclude from this data that the nanoparticles had different effects from each other.

#### Fine-particle retention during papermaking

As noted in the introduction, it has long been hypothesized that nanoparticles having a higher aspect

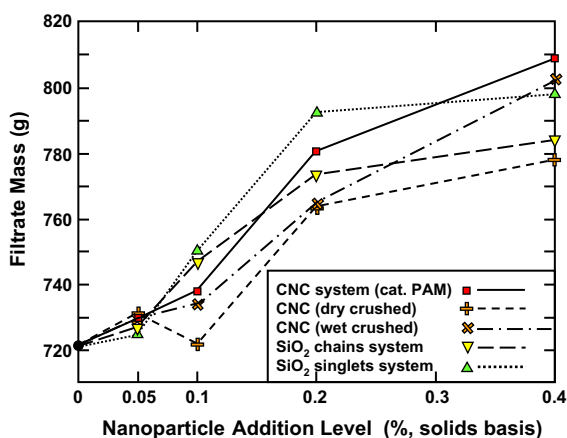


**Fig. 5** Filtrate mass after 20 s of gravity drainage, following treatment with 0.05 % poly-DADMAC, 0.05 % cPAM, and the shown levels of nanoparticles

ratio should be more effective in promoting fine-particle retention (Hubbe 2005). The approach used to examine that hypothesis, for the first time in this work, was to systematically break the CNCs into shorter pieces. The tests represented in Fig. 6 were carried out in continuous mode, meaning that there was not any interruption in agitation of the suspension (500 rpm), portions of nanoparticle suspension were added successively to the same mixture, and “zero time” corresponds to addition of just 0.05 % poly-DADMAC followed by 0.05 % cPAM.

As shown in Fig. 6, the default (unbroken) CNCs were consistently the most effective in reducing turbidity of the filtrate. Thus, following each addition of fresh CNC (see the upward-facing arrows), the lowest turbidity values were those associated with the unbroken CNC particles. However, no consistent difference was detected with respect to the turbidity-reducing ability of the two “crushed” CNCs, even though a difference in average length had been observed (see Table 1). One possible interpretation is that a certain threshold of length of CNC must be reached before greater flocculating ability can be achieved. Further study is recommended in order to provide a better test for such a hypothesis. Another issue that may be considered in future studies is whether or not the nanoparticles become aligned in

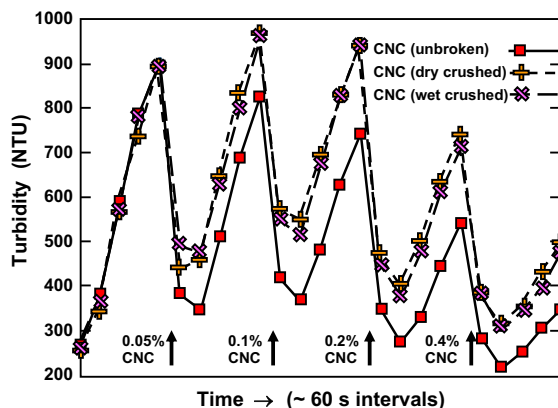


**Fig. 6** Results of continuous tests with Britt’s Dynamic Drainage/Retention Jar. Systems were treated at time zero with 0.05 % poly-DADMAC and 0.05 % cPAM. CNCs (of three types) were added at the levels shown, always just before the strong reductions in filtrate turbidity. Nanoparticle amounts shown represent the total of NPs present in the system at that point. Average values of the relative standard deviation for four independent determinations were 0.025, 0.020, and 0.018 for intact, dry crushed, and wet crushed CNCs, respectively

flow and whether such alignment affects results such as retention or flocculation.

It is also clear from Fig. 6 that turbidity of the filtrate increased rapidly with the passage of time following the most recent addition of either cPAM (after time equal to zero) or CNC (at the indicated times after each of the upward-pointing arrows). This shows that the bridging effect of the cPAM and of the cPAM/nanocellulose combinations was progressively broken down by hydrodynamic shear. However, the results in Fig. 6 show for the first time that freshly-added CNC repeatedly was able to restore the flocculating effect, holding fine particles onto cellulosic fibers. In terms of mechanisms presented earlier (Hubbe 2005), such behavior is consistent with “completion” of bridges by the freshly-added nanoparticles, which interact with adsorbed cPAM on the respective surfaces.

In theory, one end of a high-aspect-ratio nanoparticle will associate with the positively charged cPAM adsorbed on one of the surfaces, and the other end will

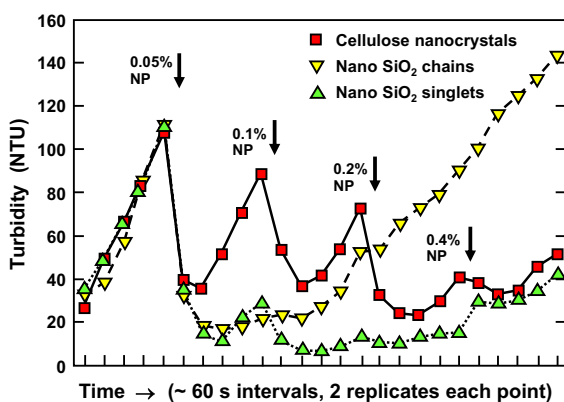


**Fig. 7** Results of continuous tests with Britt’s Dynamic Drainage/Retention Jar. Systems were treated at time zero with 0.05 % poly-DADMAC and 0.05 % cPAM. Unbroken CNCs and two types of colloidal silica were added at the levels shown. Nanoparticle amounts shown represent the total of NPs present in the system at that point. Average values of the relative standard deviation for three independent determinations were in the range of 0.1–0.5

be associated with cPAM adsorbed on another surface. Results in Fig. 6 suggest that it would be advantageous to carry out such treatment just seconds before formation of a sheet of paper, thus achieving efficient retention of the fine particles in the paper sheet as it is being formed. Indeed, such timing is consistent with modern papermaking practices. A shear-sensitive system also could allow the fiber-to-fiber attachments to become redispersed, which can be favorable to achieving uniform formation in the resulting paper (Hubbe and Wang 2002; Hubbe 2007). When comparing the three batches of CNC, the results followed the order that would be expected based on the hypothesis given earlier. In other words, the longest CNCs were the most effective, and so on.

Figure 7 compares the fine-particle retention results obtained with the default CNCs versus two types of commercially available silica nanoparticle products. As shown, both of the colloidal silica products achieved lower turbidity values in this test series in comparison to the CNCs. Moreover, both SiO<sub>2</sub> nanoparticle products achieved low turbidity values at a low addition level of the nanoparticle (each time following 0.05 % poly-DADMAC and 0.05 % cPAM additions). By contrast, an addition level of 0.5 % CNC was needed in order to achieve a turbidity value as low as about 20 NTU. Results of repeat tests with other pulp batches (not shown) indicated basically the same trends as shown in Fig. 7.

To explain these results, it was hypothesized that the surface charge density of the SiO<sub>2</sub> nanoparticles was substantially higher than that of the CNCs. Results from streaming current titrations, comparing the surface charge amounts, are shown in Table 2. Notably, the result obtained for the CNC was 0.288 meq/g, which is within the range of values obtained for CNC from the same source by Beck et al. (2015). The cited authors pretreated the material with a strong cationic exchange resin and determined charge density by a conductometric titration. On the other hand, the value obtained in the present work was

**Table 2** Comparison of the (negative) surface charge of nanoparticles (meq/g)

Description	Charge density (meq/g)		90 % confidence interval	
	Mean	SD	Lower	Upper
Intact CNC	0.288	0.028	0.255	0.320
Singlet SiO <sub>2</sub> nanoparticles	0.550	0.018	0.528	0.571
Chained SiO <sub>2</sub> nanoparticles	0.686	0.043	0.635	0.737



greater than the value 0.084 meq/g that was obtained by Araki et al. (1998, 1999) for CNC prepared in a generally similar manner. The difference might be due to differences in the source material and preparation detail of the CNC batches considered in the two studies. In addition, the methods used for evaluation of surface charge were different.

The higher relative standard deviation of replicate determinations, in Fig. 7 compared to Fig. 6, can be attributed to a shifting of the baseline from batch to batch. In each set of tests it was observed that the effects of the nanoparticles within each replication were well reproduced. However, the cationic polyacrylamide retention aid treatment by itself already produced a strong flocculating effect, which provided a slightly different starting point from which to evaluate the combined effect of the retention aid and the nanoparticle. The relative standard deviation was greater for the experiments represented in Fig. 7 because the cationic polyacrylamide treatment by itself happened to be more effective in comparison to the runs represented in Fig. 6.

As shown in Table 2, the differences in charge density of the three types of nanoparticle were in the correct order in order to account for the effects of nanoparticle dosage in Fig. 7.

Based on these results, one can understand that a greater quantity of the CNCs would be needed to balance the combined positive charge of the poly-DADMAC and cPAM already present in the system. Past work has shown that nanoparticle-based retention and dewatering systems are often optimized under charge-balanced conditions (Andersson and Lindgren 1996; Hubbe 2001).

Because the chains of  $\text{SiO}_2$  (indicated by yellow triangles in Fig. 7) had the highest negative charge density among the nanoparticle types considered, it makes sense that a high dosage of such particles would overwhelm the system with excess negative surface charge. This can explain the relatively high turbidity values for this series of tests, as can be seen in the upper right of Fig. 7. In other words, the negatively charged particles, when they were present in excess, had the effect of a dispersant. The fact that the curve rose continuously with time, when the  $\text{SiO}_2$  dosage was above 0.2 %, indicates a progressive detachment of particles with the passage of time during the continued stirring.

Confirmation of the effects just mentioned can be seen in the results obtained with the singlet  $\text{SiO}_2$  additive (green triangles in Fig. 7). Notably, that curve did not exhibit a continuous rise until a higher level of  $\text{SiO}_2$  had been reached. Such a difference is consistent with the lower charge density, compared to the  $\text{SiO}_2$  chains.

In a real paper mill it would be most common to add cPAM at just a single addition point, and this often would be shortly followed by nanoparticle addition to the mixed suspension, also at a single addition point. Because of this, some of the fine-particle retention tests were repeated in a “discontinuous” mode of addition of the poly-DADMAC, cPAM, and then each different level of nanoparticles. In other words, a new experiment was conducted for each level of nanoparticle addition. Results are shown in Fig. 8. As indicated, at the lowest dosage of nanoparticles (0.05 % on a solids basis), the nano- $\text{SiO}_2$  chains achieved the lowest turbidity (achieved in the second sets of aliquots of the replicated tests). This is consistent with the higher negative charge density of the silica nanoparticles. At the next higher level of nanoparticle addition (0.1 %), all the types of nanoparticles performed well, though the singlet  $\text{SiO}_2$  particles gave the most persistent effect in reducing the turbidity. At the highest dosage of nanoparticles, the CNCs outperformed the silica particles—showing the lowest value of turbidity

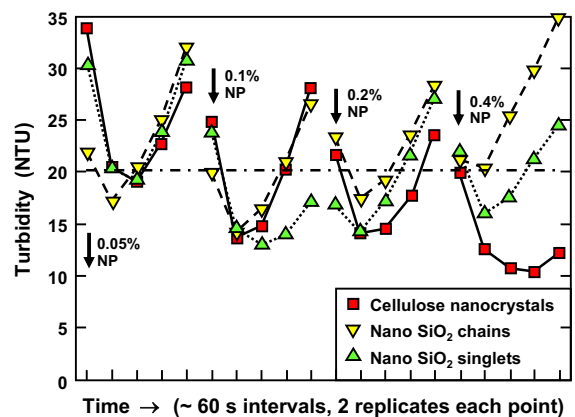


**Fig. 8** Results of discontinuous tests with Britt’s Dynamic Drainage/Retention Jar. Systems were treated at time zero with 0.05 % poly-DADMAC and 0.05 % cPAM. Unbroken CNCs and two types of colloidal silica were added at the levels shown. Average values of the relative standard deviation for four independent determinations were in the range 0.25–0.32

achieved in the whole series of tests. The fact that a greater addition of CNCs was needed to maximize its performance, relative to the SiO<sub>2</sub> products, in consistent once again with the lower negative charge density of the CNCs (Table 2).

The shear-sensitivity of the systems shown in Fig. 8 was generally in agreement with Fig. 7, indicating progressive detachment of the particles from fibers with the passage of time during continued agitation. In addition, the range of turbidity values shown in Fig. 8 was generally less than in Fig. 7. This difference is tentatively attributed to the lesser total time that any treated system was exposed to stirring (about 5 min in Fig. 8 vs. up to about 25 min in Fig. 7).

#### Fiber flocculation extent

Figure 9 reports the results for fiber flocculation tests, utilizing the potentiometric dispersion analyser (PDA) device. To summarize, addition of any of the nanoparticles to fiber suspensions that already had been treated by 0.5 % poly-DADMAC, followed by 0.05 % cPAM, generally increased the PDA output value (settings: RMS, filter), indicating an increased extent of flocculation among the fibers. In the case of SiO<sub>2</sub> nanoparticles, the largest increase in fiber flocculation was detected when the first incremental amount of 0.05 % colloidal SiO<sub>2</sub> was added to the suspension. Further incremental additions of SiO<sub>2</sub>, with continued stirring and recirculation of the suspension through the

PDA device, yielded lower levels of flocculation. In fact, at a net addition of 0.4 % colloidal silica, the PDA output values for flocculation intensity were not significantly different from the default level, representing treatment only with poly-DADMAC and cPAM. In these determinations the standard deviation of output, for specified conditions, were in the range of 0.01–0.04 PDA units. In other words, the apparent changes in flocculation extent were minor, or in a few cases insignificant, relative to the repeatability of the test. The fact that the flocculation effects were near or below the detection limit of the method can be regarded as a favorable result relative to the papermaker's usual goal of achieving a relatively uniform, unflocculated distribution of fibers within the paper product.

Results for the CNC particles, as shown in Fig. 9, generally exhibited a different trend with respect to the amount of nanoparticle added. Again, the addition of nanoparticles generally increased the value of the PDA output. However, there was no clear maximum in the results corresponding to a low nanoparticle addition level of 0.05 %. Rather, some of the highest values were obtained at an addition level of 0.2 % CNC. At the highest level of CNC addition, as in the case of SiO<sub>2</sub> nanoparticles, the PDA output was at or below the default level representing just poly-DADMAC and cPAM treatment. In other words, it took as much as four times as much CNC in some cases to achieve maximum flocculation, in comparison

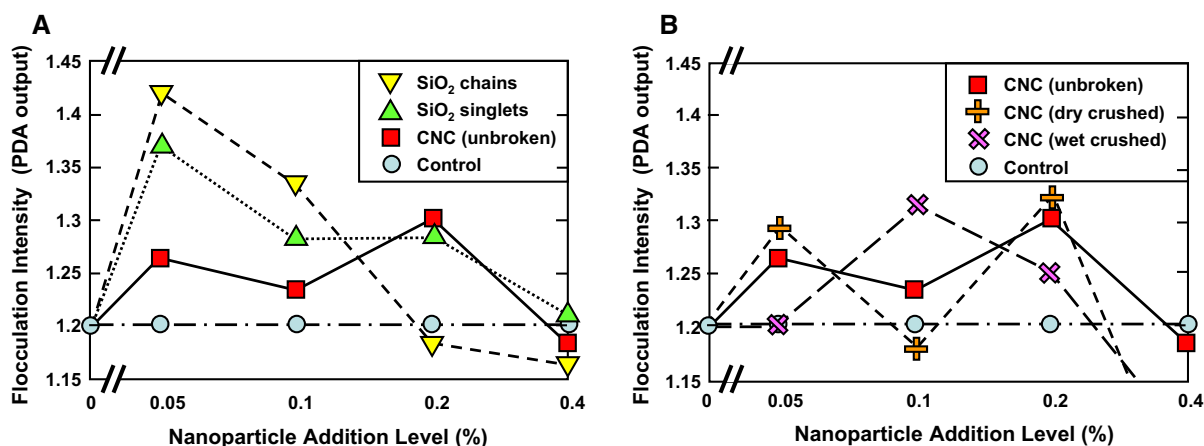


**Fig. 9** Flocculation intensity, based on PDA measurements with furnish treatment with 0.05 % poly-DADMAC, 0.05 % cPAM, and the nanoparticles of the types and amounts indicated. **a:** Comparison between effects of intact CNCs and

two types of colloidal silica. **b:** Comparison between effects of intact nanoparticles and two types of broken CNCs. Average values of the relative standard deviation for four independent determinations were in the range 0.008–0.03

to SiO<sub>2</sub> nanoparticles. To explain the fact that maximum flocculation was shifted to higher levels of nanoparticles, when using CNC, it was hypothesized that this was due to a lower surface charge density, in comparison to the same mass of SiO<sub>2</sub> nanoparticles. This hypothesis was confirmed by the test results shown in Table 2.

## Conclusions

The principal finding of this work is that longer CNCs, serving as model nanoparticles in a retention and drainage aid program, were more effective in enhancing the fine particle retention, compared to shorter CNCs. This is the first set of experiments in which it was possible to change just the length of the nanoparticles, while leaving other attributes of the system the same. The CNCs were also found to be effective in promoting dewatering, showing that indeed they can be regarded as a successful model or even a possible substitute for colloidal silica products in additive programs that involve cationic acrylamide-type retention aid addition.

Surprisingly, however, the present work did not reveal any strong advantage of structured chain-like (gel-type) colloidal silica over unstructured singlet (sol-type) colloidal silica with respect to fine-particle retention effects. A possible explanation for this is that the primary particles making up the singlets are understood to be larger than those making up the chain-like silica product. So one cannot say that “all other things are kept equal” when comparing these two colloidal silica products having different lengths.

It was also interesting to find that the drainage-boosting effects of CNCs of various length and SiO<sub>2</sub> nanoparticles of either type all were statistically indistinguishable from each other. This was despite the finding that the surface charge per unit mass was distinctly lower in the case of the CNCs, compared to the colloidal silica products. It follows that the negative charge degree of the CNCs was sufficient to achieve a sufficiently strong interaction with the cationic polyelectrolytes present in order to accomplish the strong drainage promotion, for which micro- and nanoparticle retention and drainage systems are well known.

One of the most striking and potentially advantageous attributes of the CNCs, acting as retention-promoting agents, was their sensitivity to

hydrodynamic shear. Thus, with continued stirring of the Britt Jar apparatus at 500 rpm, repeat measurements of turbidity, representing the matter in the filtrate that was not adhering to fibers, ramped steeply upwards with time during continued stirring. Subsequent incremental additions of CNCs were able to reset the turbidity values to low values, and the pattern was repeated. Such transient, relatively weak bridging effects demonstrated by the CNCs used in this work suggest a potential to achieve favorable combinations of paper uniformity and retention of fine particles. This possibility is also supported by the low levels of fiber floc formation that were observed with the PDA test results. Various questions related to charge interactions will be pursued in ongoing research.

**Acknowledgments** The authors are grateful for support from North Carolina State University for an award of an Undergraduate Research Grant to Caryn Peksa in 2014, for the Buckman Foundation, for support of undergraduate research of Connor Lenze in 2015, and for funding from Northwestern Polytechnical University in Xian, China to support the work of visiting scholar, Dr. Weimin Sun.

## References

- Abitbol T, Palermo A, Moran-Mirabel JM, Cranston ED (2013) Fluorescent labeling and characterizations of cellulose nanocrystals with varying charge contents. *Biomacromolecules* 14:3278–3284
- Andersson K, Lindgren E (1996) Important properties of colloidal silica in microparticulate systems. *Nordic Pulp Paper Res J* 11(1):15–21
- Andersson K, Sandström A, Ström J, Barla P (1986) The use of cationic starch and colloidal silica to improve the drainage characteristics of kraft pulps. *Nordic Pulp Paper Res J* 1(2):26–30
- Araki J, Wada M, Kuga S, Okano T (1998) Flow properties of microcrystalline cellulose suspension prepared by acid treatment of native cellulose. *Colloids Surf A Physicochem Eng Aspects* 142(3):75–82
- Araki J, Wada M, Kuga S, Okano T (1999) Influence of surface charge on viscosity behavior of cellulose microcrystal suspension. *J Wood Sci* 45(3):258–261
- Asselman T, Garnier G (2001) The flocculation mechanism of microparticulate retention aid systems. *J Pulp Paper Sci* 27(8):273–278
- Beck S, Méthot M, Bouchard J (2015) General procedure for determining cellulose nanocrystal sulfate half-ester content by conductometric titration. *Cellulose* 22(1):101–116
- Breese J (1994) Interactive papermaking chemistry provides machine rebuild options. *Pulp Paper* 68(4):91–92 (95–97)
- Britt KW (1973) Retention of additives during sheet formation. *Tappi* 56(3):83–86

- Britt KW, Unbehend JE (1976) New methods for monitoring retention. *Tappi* 59(2):67–70
- Burgess MS, Phipps JS (2000) Flocculation of PCC induced by polymer/microparticle systems: floc characteristics. *Nordic Pulp Paper Res J* 15(5):572–578
- Burgess MS, Curley JE, Wiseman N, Xiao H (2002) On-line optical determination of floc size. Part 1. Principles and techniques. *J Pulp Paper Sci* 28(2):63–65
- Carlson U (1990) Some aspects of microparticle flocculation. In: *The world pulp & paper week: EUCEPA XXIV, Paper Technology, Stockholm, May*, pp. 161–171
- Carr D (2005) Nanoparticulates on colloidal retention. In: *Wet end chemistry*, Pira International, Boston, MA, October, Paper 9
- Habibi Y (2010) Cellulose nanocrystals: chemistry, self assembly, and applications. *Chem Rev* 110:3479–3500
- Hangen M, Tokarz M (2002) The third generation of nanoparticle retention systems. In: *Scientific & technical advances in wet end chemistry*, Pira International, Leatherhead, UK, Paper 9
- Harms M (1998) Second generation microparticle systems. *Wochenbl Papierfabr* 126(19):922–924
- Honig DS, Farinato RS, Jackson LA (2000) Design and development of the micropolymer system: an ‘organic microparticle’ retention/drainage system. *Nordic Pulp Paper Res J* 15(5):536–544
- Hubbe MA (2000) Reversibility of polymer-induced fiber flocculation by shear. 1. Experimental methods. *Nordic Pulp Paper Res J* 15(5):545–553
- Hubbe MA (2001) Reversibility of polymer-induced fiber flocculation by shear. 2. Multi-component chemical treatments. *Nordic Pulp Paper Res J* 16(4):369–375
- Hubbe MA (2005) Microparticle programs for drainage and retention. In: Rodriguez JM (ed) *Micro and Nanoparticles in Papermaking*. TAPPI Press, Atlanta, pp 1–36 **Chapter 1**
- Hubbe MA (2007) Flocculation and redispersion of cellulosic fiber suspensions. A review of effects of hydrodynamic shear and polyelectrolytes. *BioResources* 2(2):296–331
- Hubbe MA, Wang F (2002) Where to add retention aid: issues of time and shear. *Tappi J* 1(1):28–33
- Langley JG, Litchfield E (1986) Dewatering aids for paper application. In: *Proceedings on TAPPI 1986 Papermakers Conference*, pp 89–92
- Larson RG (2005) The rheology of dilute solutions of flexible polymers: progress and problems. *J Rheol* 49(1):1–70
- Main S, Simonson P (1999) Retention aids for high-speed paper machines. *Tappi J* 82(4):78–84
- Moffett RH (1994) On-site production of a silica-based microparticulate retention and drainage aid. *Tappi J* 77(12):133–138
- Reiner RS, Rudie AW (2013) Process scale-up of cellulose nanocrystal production to 25 kg per batch at the Forest Products Laboratory. In: Postek MT, Moon RJ, Rudie AW, Bilodeau MA (eds) *Production and applications of cellulose nanomaterials*. TAPPI Press, Atlanta, pp 21–24
- Sampson WW (1997) The interdependence of sheet structure and drainage. *Paper Technol Ind* 38(8):45–50
- Sampson WW, Kropholler HW (1995) Batch-drainage curves for pulp characterization. Part 1. Experimental. *Tappi J* 78(12):145–151
- Sang YZ, McQuaid M, Englezos P (2012) Pre-flocculation of precipitated calcium carbonate filler by cationic starch for highly filled mechanical grade paper. *BioResources* 7(1):354–373
- Sears GW (1956) Determination of specific surface area of colloidal silica by titration with sodium hydroxide. *Anal Chem* 28(12):1981–1983
- Sridhar T, Tirtaatmadja V, Nguyen DA, Gupta RK (1991) Measurement of extensional viscosity of polymer solutions. *J NonNewton Fluid Mechan* 40(3):271–280
- Swerin A, Sjödin U, Ödberg L (1993) Flocculation of cellulosic fibre suspensions by model microparticulate retention aid systems. *Nordic Pulp Paper Res J* 8(4):389–398
- Swerin A, Glad-Nordmark G, Sjödin U (1995) Silica based microparticulate retention aid systems. *Paperi Puu* 77(4):215–221
- Swerin A, Glad-Nordmark G, Ödberg L (1997) Adsorption and flocculation in suspensions by two cationic polymers—Simultaneous and sequential addition. *J Pulp Paper Sci* 23(8):J389–J393
- Wågberg L, Björklund M, Åsell I, Swerin A (1996) On the mechanism of flocculation by microparticle retention aid systems. *Tappi J* 79(4):157–164
- Xu QH, Li WG, Cheng ZL, Yang G, Qin MH (2014) TEMPO/NaBr/NaClO-mediated oxidation of nanocrystalline cellulose and its microparticulate retention system with cationic polyacrylamide. *BioResources* 9(1):994–1006
- Zhang W, Johnson RK, Lin ZY, Cody LC, Audrey ZS, Rennecker S (2013) In situ generated cellulose nanoparticles to enhance the hydrophobicity of paper. *Cellulose* 20:2935–2945